1st Biannual Post Graduate Conference
7th-10th May 2014, Seri Iskandar, Perak

Flow Characteristics of 3-D Turning Diffuser

Normayati Nordin
Faculty of Mechanical and Manufacturing Engineering
Universiti Tun Hussein Onn Malaysia
Batu Pahat, Malaysia
mayati@uthm.edu.my

Zainal Ambri Abdul Karim
Department of Mechanical Engineering
Universiti Teknologi Petronas
Tronoh, Malaysia
ambri@petronas.com.my

Safiah Othman
Faculty of Mechanical and Manufacturing Engineering
Universiti Tun Hussein Onn Malaysia
Batu Pahat, Malaysia
safiah@uthm.edu.my

Vijay R. Raghavan
OYL Research & Development Centre
OYL Research & Development Sdn Bhd
Sungai Buloh, Malaysia
vijay@oyl.com.my

***Abstract*— It is often necessary in fluid flow systems to simultaneously decelerate and turn the flow. This can be achieved by employing turning diffusers in the fluid flow systems. The flow through a turning diffuser is complex, apparently due to the expansion and inflexion introduced along the direction of flow. The flow characteristics of 3-D turning diffuser by means of varying inflow Reynolds number are presently investigated. The flow characteristics within the outlet cross-section and longitudinal section were examined respectively by the 3-D stereoscopic PIV and 2-D PIV. The flow uniformity is affected with the increase of inflow Reynolds number due to the dispersion of the core flow throughout the outlet cross-section. It becomes even worse with the presence of secondary flow, 22% to 27% of the mean outlet velocity. The flow separation takes place within the inner wall region at the point very close to the outlet edge and the secondary flow vortex occurs dominantly within half part of the outlet cross-section.**

Keywords—turning diffuser; flow characteristics; particle image velocimetry (PIV)

I. INTRODUCTION

It is often necessary in fluid flow systems to simultaneously decelerate and turn the flow. This can be achieved by employing turning diffusers in the fluid flow systems. A turning diffuser is characterised by its expansion directions into two types, namely, two dimensional (2-D) turning diffuser and three-dimensional (3-D) turning diffuser [1, 2, 3]. A geometric layout of a 90^o turning diffuser is shown in Fig. 1. A 2-D turning diffuser expands its cross-section in either x-y or y-z axis plane, whereas a 3-D turning diffuser expands its cross-section in both x-y and y-z planes.

Chong et al. [4] designed a 90^o turning diffuser with quadrants of circles at both the inner wall and centerline. The outer wall was shaped using circular arcs with the centers placed along the centerline and the circumferences tangent to the inner wall. It was designed such that equal area distributions were established between the inner and outer

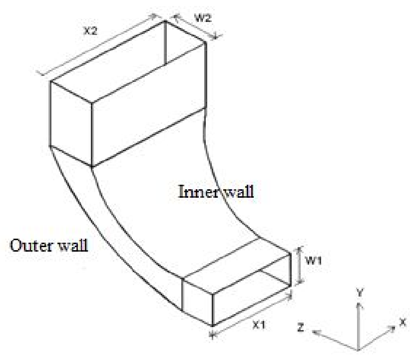

Fig. 1. A geometric layout of a 90^o turning diffuser

wall passages relative to the centerline. The gross geometry of a turning diffuser could be described in terms of four parameters, namely, the inner wall length to the inlet throat width ratio (L_{in}/W_1), the outlet area to the inlet area ratio (AR) , the outlet-inlet configurations (W_2/W_1, X_2/X_1) and the turning angle ($\Delta\phi$) [5].

The flow through a 90^o turning diffuser is complex, apparently due to the expansion and sharp inflexion introduced along the direction of flow. The inner wall is subjected to curvature-induced effects where under a strong adverse pressure gradient, the boundary layer on the inner wall is likely to separate, and the core flow tends to deflect toward the outer wall region [2, 6]. Flow separation is basically undesirable as it would decrease the core flow area, induce the presence of secondary flow vortices and ultimately affect the flow uniformity [4]. The flow uniformity index (σ_{out}) is used to measure the extent of dispersion of local oulet velocity from the mean outlet velocity. The σ_{out} was strongly dependent on the dispersion of core flow, σ_y and the presence of secondary flow, S_{out} throughout the outlet cross-section [7].

In the present work, the flow characteristics of 3-D turning diffuser of $\Delta\phi$= 90°, AR= 2.16, W_2/W_1=1.440, X_2/X_1=1.500 and L_{in}/W_1= 3.970 are experimentally investigated. The operating condition is varied within the range of inflow Reynolds number, Re_{in}= 5.786E+04 - 1.775E+05.

II. Instrumentation And Measurement Setup

The test rig shown in Fig. 2 was developed. A centrifugal blower controlled using a 3-phase inverter and calibrated previously by [8] was installed at the upstream end. The rig was incorporated with several wind tunnel features to produce a fully developed flow at the diffuser entrance [9]. The test section, with inlet cross-section of 13 cm x 5 cm and hydrodynamic entrance length of 28D_h featured no fittings.

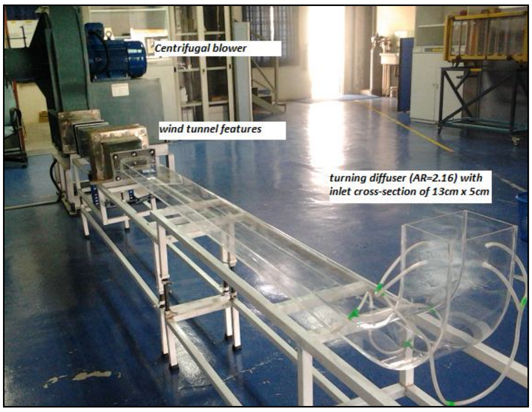

Fig. 2. Test rig

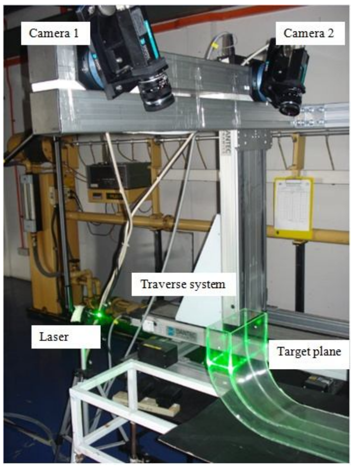

Fig. 3. 3-D stereoscopic PIV setup

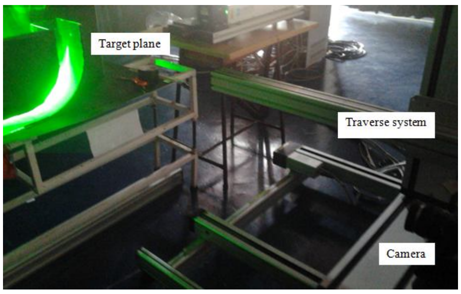

Fig. 4. 2-D PIV setup

The outlet flow uniformity was examined using a 3-D stereoscopic PIV shown in Fig. 3. In order to allow shots of the entire outlet plane to be taken, the cameras were mounted at 30° angle each and leveled up within a satisfied-calibrated distance on the top of the target plane. A 2-D PIV was used to examine the flow characteristic at the center plane within the longitudinal section, with the camera arranged to be perpendicular to the target plane shown in Fig. 4. The results obtained were verified [10].

The flow uniformity index (σ_{out}) was evaluated by calculating the mean standard deviation of outlet velocity. The least absolute deviation corresponds to the greatest uniformity of flow [12]:

$$\sigma_{out} = \sqrt{\frac{1}{N-1}\sum_{i=1}^{N}(V_i - V_{outlet})^2} \qquad (1)$$

where,

N= number of measurement points
V_i = local outlet air velocity (m/s)
V_{out} = mean outlet air velocity (m/s)

The dispersion of core flow (σ_y) was evaluated by calculating the standard deviation of axial velocity at the outlet [11]:

$$\sigma_y = \sqrt{\frac{1}{N-1}\sum_{i=1}^{N}(V_y - V_{yavg})^2} \qquad (2)$$

where,

V_y = velocity in y-direction (m/s)
$V_{y\,avg}$ = average velocity in y-direction (m/s)

Secondary flow index (S_{out}) represents the percentage of secondary flow at the outlet. The outlet velocity is considered uniform only if secondary flow magnitude at the outlet is less than 10% of the mean outlet velocity [7]:

$$S_{out} = \left(\sum_{i=1}^{N}\sqrt{V_x^{\,2} + V_z^{\,2}}\right)\frac{1}{N \times V_{out}} \qquad (3)$$

where,

V_x = velocity in x-direction (m/s)
V_z = velocity in z-direction (m/s)

III. Results Analysis And Discussion

Contours as depicted in Fig. 5 exhibit the characteristic of the outlet flow. The core flow that is in y-direction is represented by colour-code. Whereas, the secondary flow resulting of the flows in x- and z-direction is represented by vector-arrows. In general, each contour shares almost the same characteristic with the rapid flow mostly occurring within the outer wall region and the flow deficit is seen to happen within the inner wall region. There are presences

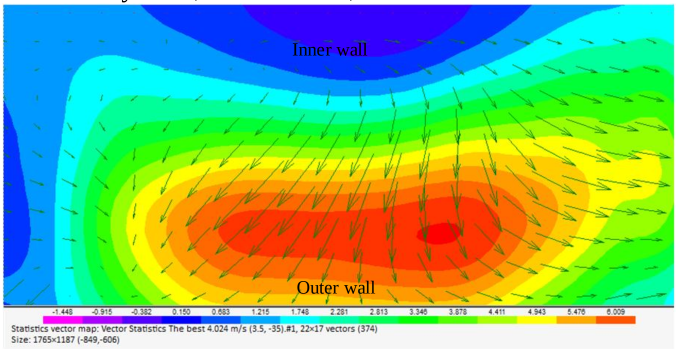

(a)

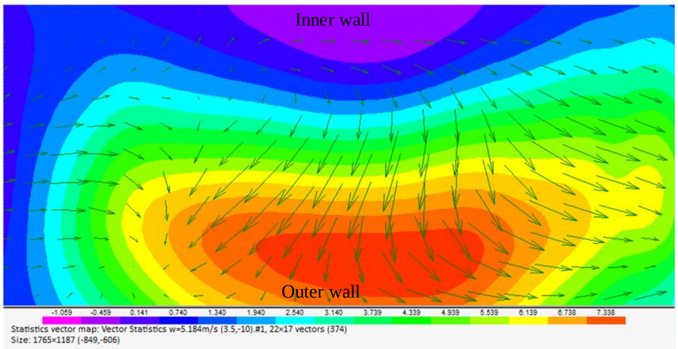

(b)

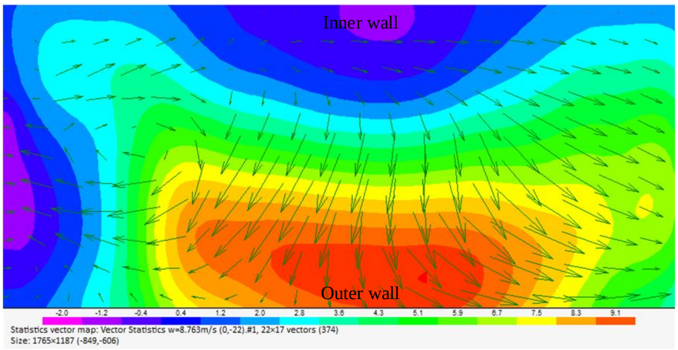

(c)

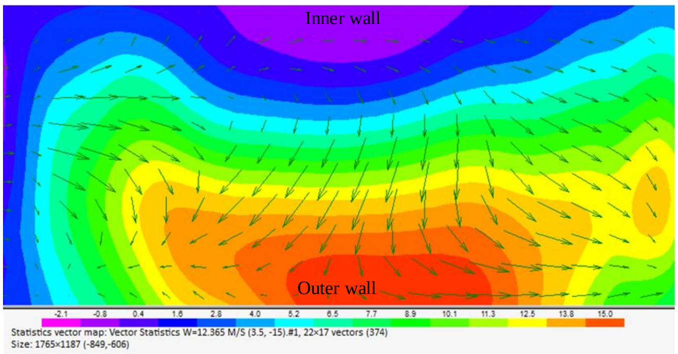

(d)

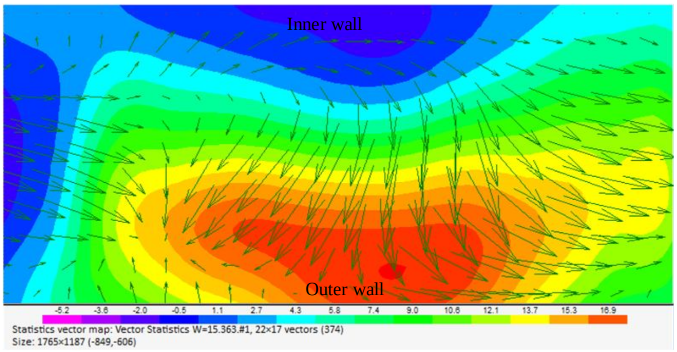

(e)

Fig. 5. Characteristic of the core flow, V_y (represented by color-coded) and the resultant of secondary flows, V_x and V_z (represented by arrows) at the outlet by varying (a) Re_{in}=5.786E+04 (b) 6.382E+04 (c) 1.027E+05 (d) 1.397E+05 (e) 1.775E+05

of swirling secondary flow vortices throughout the outlet cross-section and reverse core flows close to the inner wall region in each case.

Velocity profiles are extracted across the center of the turning diffuser outlet at two (2) different planes as shown in Fig. 6. As depicted in Fig. 7, the profiles are obtained to be asymmetric in each case. In Plane A, the flows deflect much toward the outer wall due to the existence of reverse core flows within the inner wall region. In Plane B, the secondary flow vortex occurs dominantly within half part of the outlet, i.e. left side causing the flow area in that particular region is to decrease.

The σ_{out} is affected with the increase of Re_{in} as indicated in TABLE I mainly because of the dispersion of the core flow throughout the outlet cross-section, σ_y. It becomes even worse with the presences of the secondary flow, S_{out}= 22% to 27% of the mean outlet velocity. The secondary flow vortices throughout the outlet cross-section together with the excessive flow separation within the inner wall region may occur under a very strong pressure gradient and these not only incur unfavorable flow performance but also considerable losses associated with form drag [13, 14].

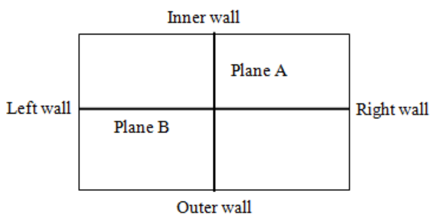

Fig. 6. Velocity profile planes across the center of turning diffuser outlet

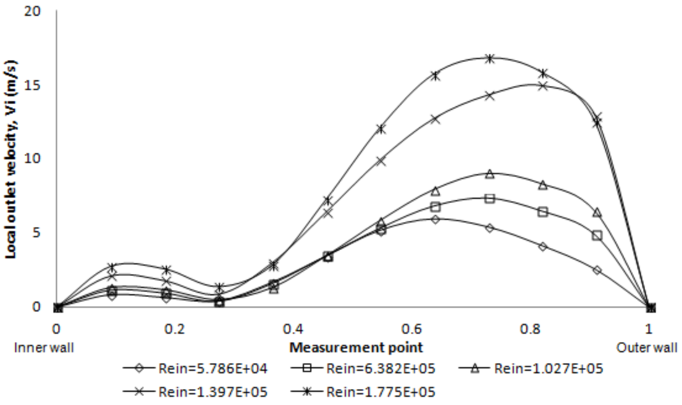

(a)

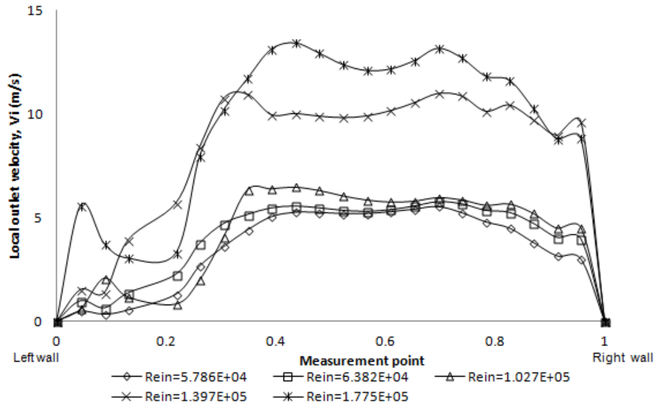

(b)

Fig. 7. Velocity profiles at (a) Plane A and (b) Plane B

TABLE I. FLOW PFERFORMANCE INDEXES

Re_{in}	σ_{out}	σ_y	S_{out}
5.786E+04	1.82	1.90	0.268
6.382E+04	2.25	2.40	0.223
1.027E+05	2.70	2.93	0.243
1.397E+05	4.64	5.01	0.236
1.775E+05	5.05	5.74	0.254

Vector plots, as in Fig. 8, demonstrate the flow structures within the longitudinal section of turning diffuser taken at the center plane. Since the flow structures of each case are almost the same, in order to avoid repetition, only the flow structures of minimum and maximum Re_{in} are included in the paper. The boundary layer in each case separates from the inner wall almost at the same point which is close to the outlet edge, $S= 0.9L_{in}/W_1$.

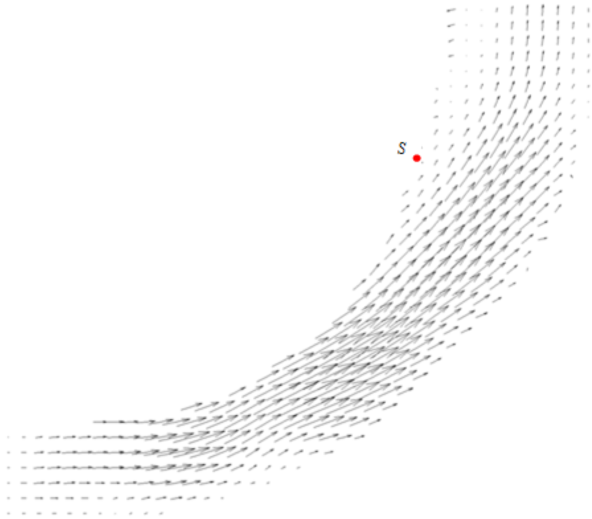

(a)

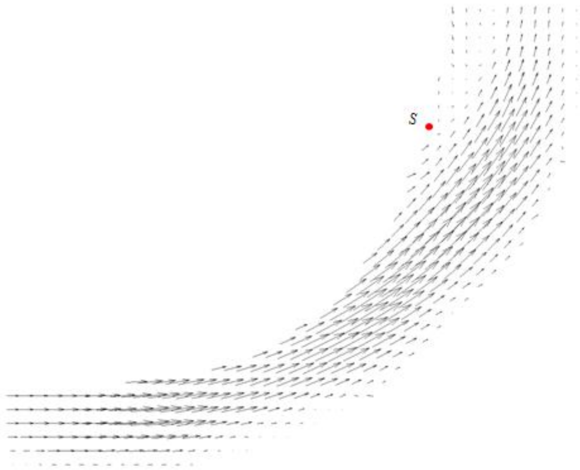

(b)

Fig. 8. Flow structures within the longitudinal section of turning diffuser (a) Re_{in}=5.786E+04 (b) 1.775E+05

IV. CONCLUSION

In conclusion, the current work managed to investigate the flow characteristics of 3-D turning diffusers by means of varying Re_{in}= 5.786E+04 - 1.775E+05. The flow uniformity is affected with the increase of Re_{in} mainly because of the dispersion of the core flow throughout the outlet cross-section. It becomes even worse with the presences of secondary flow, 22% to 27% of the mean outlet velocity. The secondary flow vortex occurs dominantly within half part of the outlet, i.e. left side causing the flow area in that particular region is to decrease. The flow separation takes place within the inner wall region close to the outlet edge of approximately $0.9L_{in}/W_1$.

ACKNOWLEDGMENT

This work was financially supported by the Fundamental Research Grant Scheme (FRGS) of the Ministry of Higher Education, Malaysia. The experimental work was conducted in the Aerodynamics Laboratory, Universiti Tun Hussein Onn Malaysia (UTHM).

REFERENCES

[1] G. Gan and S.B. Riffat, “Measurement and computational fluid dynamics prediction of diffuser pressure-loss coefficient,” *Applied Energy*, vol. 54(2), pp. 181-195, 1996.

[2] R.K. Sullerey, B. Chandra, and V. Muralidhar, "Performance comparison of straight and curved diffusers," *J. of Def. Sci.*, vol. 33, pp. 195-203, 1983.

[3] N. Nordin, V.R. Raghavan, S. Othman and Z.A.A. Karim,“Compatibility of 3-D turning diffusers by means of varying area ratios and outlet-inlet configurations", *ARPN Journal of Engineering and Applied Sciences*, Vol. 7, No. 6, pp 708-713, 2012.

[4] T.P. Chong, P.F. Joseph and P.O.A.L. Davies, “A parametric study of passive flow control for a short, high area ratio 90 deg curved diffuser,” *J. Fluids Eng.*, vol. 130, 2008.

[5] C.J. Sagi and J.P. Johnson, “The design and performance of two-dimensional, Curved Diffusers,” *J. Basic Eng. ASME*, vol. 89, pp. 715-731, 1967.

[6] N. Nordin, V. R. Raghavan, S. Othman and Z. A. A. Karim, “Numerical investigation of turning diffuser performance by varying geometric and operating parameters”, *Applied Mechanics and Materials Journal*, Vol. 229-231, pp. 2086-2093, 2012.

[7] M. K. Gopaliya, P. Goel, S. Prashar, and A. Dutt, "CFD Analysis of performance characteristics of S-shaped diffusers with combined horizontal and vertical offsets," *Computer & fluids*, vol. 40, pp. 280-290, 2011.

[8] N. Nordin, Z.A.A. Karim, S. Othman and V.R. Raghavan, “Design & development of low subsonic wind tunnel for turning diffuser application”, *Advanced Material Research Journal*, Vol. 614-615, pp. 586-591, 2013.

[9]N.Nordin, Z.A.A. Karim, S.Othman and V.R. Raghavan, “Verification of fully developed flow entering diffuser and particle image velocimetry procedures”, *Applied Mechanics and Materials Journal*, Vol. 465-466, pp. 1352-1356, 2014.

[10] N. Nordin, S. Othman, V.R. Raghavan and Z.A.A. Karim, “Verification of 3-D stereoscopic PIV operation and procedures”, *International Journal Engineering and Technology IJET/IJENS*, , Vol. 12, Issue 4, pp. 19-26, 2012.

[11] M.K. Gopaliya, M. Kumar, S. Kumar, and S. M. Gopaliya, "Analysis of performance characteristics of S-shaped diffuser with offset," *Aerospace Science & Tech.*, vol. 11, pp. 130-135, 2007.

[12] W.A. El-Askary and M. Nasr, “Performance of a bend diffuser system: Experimental and numerical studies,” *Computer & Fluids*, vol. 38, pp. 160-170, 2009.

[13] N.Nordin, Z,A.A. Karim, S.Othman and V.R. Raghavan, The performance of turning diffusers at various inlet conditions, *Applied Mechanics and Materials Journal*, Vol. 465-466, pp. 597-602, 2014.

[14] N.H.N. Seth, N.Nordin, S.Othman and V.R. Raghavan, Investigation of flow uniformity and pressure recovery in a turning diffuser by means of baffles, *Applied Mechanics and Materials Journal*, Vol. 465-466, pp. 526-530, 2014.